Radiophysics and Quantum Electronics, Vol. 50, No. 4, 2007

SOLUTION OF A SUBSURFACE RADIO-IMAGING INVERSE PROBLEM IN THE APPROXIMATION OF A STRONGLY REFRACTIVE MEDIUM

V. P. Yakubov * **and D. Ya. Sukhanov**

UDC 621.396.962.21

In the approximation of a strongly refractive medium, we solve the inverse problem of subsurface-radar imaging of buried inhomogeneities using data of multiposition ultra-wideband radio sounding. The fast Fourier transform is used for synthesizing a large aperture with focusing. A mathematical model of the proposed subsurface-imaging system is presented and its accuracy is estimated. The feasibility of the proposed method is confirmed by numerical simulations and model laboratory experiments.

1. INTRODUCTION

At present, detection of dielectric buried land inhomogeneities becomes a topical problem. First of all, this is related to the wide use of plastic antipersonnel land mines, the detection of which by means of conventional induction-type mine detectors is impossible. The most promising approach to detection of buried dielectric objects is the use of ground penetrating radars. However, the theoretical description of the radio sounding of ground-buried objects is complicated by difficulties in the description of the interaction of radio waves with the medium and the scattering inhomogeneities. Besides, there occur the radio-wave refraction at the interface of the media, strong attenuation of radio waves in the ground, dispersion effects, and multiple scattering.

A wideband synthetic aperture radar (SAR) is a convenient tool for studying buried objects. In this method of sounding, the scattered radiation provides the most complete data on the scattering inhomogenities in the medium. To obtain useful information from the scattering data, the inverse problem of subsurface radio sounding should be solved, i.e., the distribution of the inhomogeneities in the medium should be reconstructed using the data on the radiation sources and the scattered field.

At present, numerous methods are available for the solution of the inverse problem of subsurface imaging on the basis of the scattered field parameters obtained by the SAR method [1–7]. In most of such methods, the scattered field is measured by moving a system of omnidirectinal transmitting and receiving antennas in the horizontal plane at a fixed altitude above the ground surface. The sounding is performed using pulsed ultra-wideband radiation. If a point scatterer is located in the medium, the dependence of the time delay of the scattered pulse on the coordinates of the antenna system has the form of the diffraction hyperbola. The shape and position of the diffraction hyperbola give information on the scatterer coordinates. In the case of distributed scatterers, the method of selective summation in the time domain over the diffraction hyperbola is used, which is known as the migration method. In practice, the pulse radiation is difficult to use, so that alternatively monochromatic signals swept in a wide frequency band are often employed. Then the Fourier transform is applied in order to pass from the frequency domain to

* yvlp@mail.tsu.ru

Tomsk State University, Tomsk, Russia. Translated from Izvestiya Vysshikh Uchebnykh Zavedenii, Radiofizika, Vol. 50, No. 4, pp. 329–338, April 2007. Original article submitted October 11, 2005; accepted April 13, 2007.

the time domain. The so-transformed data are equivalent to the results of sounding the medium by pulse signals.

In [2] the three-dimensional focusing by the time-domain migration method is discussed for a SAR-system moved in the horizontal plane and operated in the frequency range 2–6 GHz. It is shown that the image of the buried object can be obtained using an approximate determination of delay times of the scattered signals. A technique based on the processing of impulse responses of a ground penetrating radar to point scatterers is presented in [8], in which the Hough transform is applied to determine the position of the object from the shape of the diffraction hyperbola.

A method of the scattered-signal focusing in the frequency domain (taking into account the radio-wave refraction at the medium interface in accordance with Snell's law) is considered in [3] for one-dimensional scanning by an antenna system. This approach admits using fast algorithms based of the fast Fourier transform (FFT). However, the necessity to perform the three-dimensional focusing significantly slows down the processing of the measurement data. Another example of successful use of the SAR technology with the frequency scanning is given in [1], in which a method of two-dimensional angular scanning by an antenna system in the upper half-space is considered with allowance for the dispersion effects during the wave refraction and attenuation in the sounded medium. The data processing is performed using the spatial matched filtering and focusing of the radiation to each point of the lower half-space. Sequential scanning of the focusing point ensures the three-dimensional reconstruction of the inhomogeneities under the interface of the media. A test experiment was performed with metal spheres of 7.62 cm in diameter embedded in wet sand at a depth of 27–67 cm in a cylindrical container of 2 m in diameter. The operating range of the sounding frequencies was 2–6 GHz. The experiment confirmed the good robustness of the method. However, the signal processing in the experiment required about 4 hours even when using a 64-bit high-performance processor. The spatial resolution achieved in the experiment was of the order of the sphere size.

In [6], the inverse problem is solved using the diffraction tomography method in the single-scattering approximation. The interaction of the radiation and the medium interface is taken into account in the spatial spectrum of plane waves of the transmitting and receiving antennas. The analytical solution of the direct problem is sought using the spectral decomposition of the radiation into plane waves for large depths in the approximation of a strongly refractive medium. The solution of the inverse problem in the far-zone approximation is then reduced to a convolution integral. The results of numerical simulation showed the workability of the described method for detection of dielectric inhomogeneities, but no results were reported for processing actual experimental data by this algorithm.

In [7], a new method for fast reconstruction of dielectric inhomogeneities, based on the approximation of strong refraction of waves in the medium and a large-aperture synthesis technique, is briefly described. In the present work, we present a detailed description of this method and obtain the estimate of its accuracy for the case of 3D-reconstruction of inhomogeneities in the medium. Theoretical conclusions are compared with the results of numerical simulations and physical experiments.

2. THE INSTRUMENT FUNCTION

To develop a convenient mathematical model, we adopt several simplifications. We assume that the ground surface is flat and the inhomogeneities in the lower half-space V_1 are characterized by a small relative perturbation $\Delta\varepsilon(\mathbf{r})$ of the dielectric permittivity. The scattering of radio waves by the inhomogeneities is considered in the scalar approximation of single scattering (at first, in the frequency-domain representation). Let us assume for simplicity that the transmission and reception points coincide with the point $\mathbf{r}_0 = (x_0, y_0, h)$, which can move at the height $h = \text{const}$ in air over the interface between the media (Fig. 1). The horizontal position of this point is described by the vector $\boldsymbol{\rho}_0 = (x_0, y_0)$.

On the assumption of single scattering, one can write the following expression for the complex amplitude of the field with frequency f at the reception point $\mathbf{r}_0$:

$$E(\boldsymbol{\rho}_0, f) = k_1^2 \iiint\limits_{V_1} \Delta\varepsilon(\boldsymbol{\rho}_1, z_1) G^2(\boldsymbol{\rho}_1 - \boldsymbol{\rho}_0, z_1)\, \mathrm{d}^2\boldsymbol{\rho}_1\, \mathrm{d}z_1, \tag{1}$$

where

$$G(\boldsymbol{\rho}, z) = \int\limits_{-\infty}^{+\infty}\!\!\int \frac{iT(\mathbf{k}) \exp[i\,(\mathbf{k}_\perp \boldsymbol{\rho} + k_z h + k_{1z} z)]}{2\,(2\pi)^2\, k_z}\, \mathrm{d}^2\mathbf{k}_\perp \tag{2}$$

is the Green's function describing the field in the lower half-space due to a point source located in the upper half-space, $k = 2\pi f/c$ is the wave number in free space, c is the speed of light in vacuum, and $T(\mathbf{k})$ is the Fresnel transmission coefficient of the medium interface for the spectral components of plane waves. The quantities $k_z = \sqrt{k^2 - k_\perp^2}$ and $k_{1z} = \sqrt{k^2 n^2 - k_\perp^2}$ are the vertical components of the wave vectors for the incident ($\mathbf{k} = (\mathbf{k}_\perp, k_z)$) and refracted ($\mathbf{k}_1 = (\mathbf{k}_\perp, k_{1z})$) plane waves in the upper and lower half-spaces, respectively, and n is the refractive index of the sounded medium. The current position of the scattering point is given by the vector $\mathbf{r}_1 = (x_1, y_1, z_1) \equiv (\boldsymbol{\rho}_1, z_1)$, and its projection onto the interface between the media, by the vector $\boldsymbol{\rho}_1 = (x_1, y_1)$.

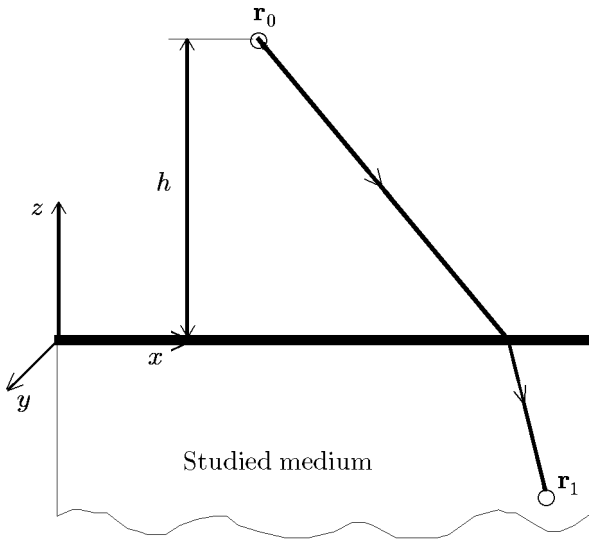

Fig. 1. The path of wave refraction.

Equation (1) takes into account the effect of scattering by inhomogeneities in the lower half-space and neglects the reflection from the interface of the media. Unlike the well-known Born approximation, Eq. (1) accounts for the refraction accompanying the transmission of the wave from one medium to another. Note that although the Green's function $G(\boldsymbol{\rho}, z)$ is rigorously written, it cannot be calculated in closed form analytically and only its asymptotic can be found, for example, in the the geometrical-optics approximation [9].

It is assumed that the measurements at the frequency $f = ck/(2\pi)$ give the distribution of the scattered field $E(\boldsymbol{\rho}_0, f)$ over a certain plane above the surface of the medium. The use of the synthetic-aperture radar method makes it possible to reconstruct the spatial distribution of inhomogeneities in the bulk of the medium by the inversion of integral (1). To find this distribution, we focus field (1) to a certain point $\boldsymbol{\rho}_\mathrm{F}$ at the interface of the media. As is known, the focusing procedure consists in the in-phase summation of complex amplitudes of the scattered field at the chosen focus point. To ensure such a summation, it is necessary to compensate for the phase increments accumulated between the transmitting antenna and the focus point and then between the focus point and the receiving antenna. The result of the scattered-field focusing to the point $\boldsymbol{\rho}_\mathrm{F}$ at the surface can be written as the convolution integral:

$$F(\boldsymbol{\rho}_\mathrm{F}, f) = \iint\limits_{S} E(\boldsymbol{\rho}_0, f) M(\boldsymbol{\rho}_\mathrm{F} - \boldsymbol{\rho}_0, f)\, \mathrm{d}^2\boldsymbol{\rho}_0,$$

where $M(\boldsymbol{\rho}, f) = \exp[-ik\,(2\sqrt{\boldsymbol{\rho}^2 + h^2})]$ is the simplest form of the corresponding weight function of the focusing and integration is performed over the entire observation plane S which represents the synthetic-aperture plane.

Allowing for Eq. (1), the focused field can be rewritten in the form

$$F(\boldsymbol{\rho}_\mathrm{F}, f) = \iiint\limits_{V_1} \Delta\varepsilon(\boldsymbol{\rho}_1, z_1) Q(\boldsymbol{\rho}_1, \boldsymbol{\rho}_\mathrm{F}, z_1, f)\, \mathrm{d}\mathbf{r}_1, \tag{3}$$

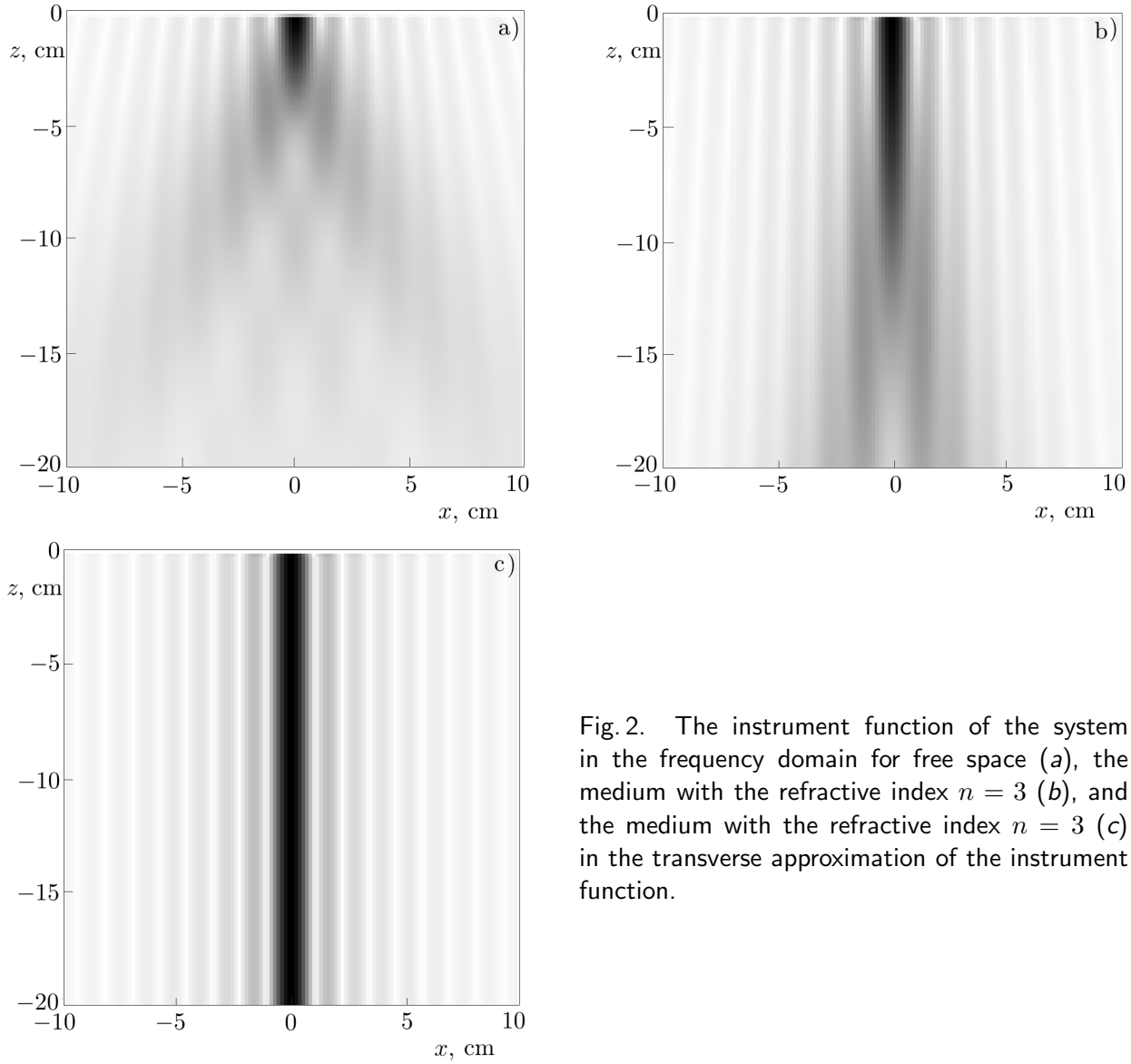

Fig. 2. The instrument function of the system in the frequency domain for free space (*a*), the medium with the refractive index $n = 3$ (*b*), and the medium with the refractive index $n = 3$ (*c*) in the transverse approximation of the instrument function.

where

$$Q(\boldsymbol{\rho}_1, \boldsymbol{\rho}_\mathrm{F}, z_1, f) = k_1^2 \iint\limits_S G^2(\boldsymbol{\rho}_1 - \boldsymbol{\rho}_0, z_1) M(\boldsymbol{\rho}_\mathrm{F} - \boldsymbol{\rho}_0, f)\, \mathrm{d}\boldsymbol{\rho}_0 \tag{4}$$

is the response of the system to a point scatterer located at the point $\mathbf{r}_1$, i.e., it represents the instrument function of the system at frequency f for the focusing to the point $\boldsymbol{\rho}_\mathrm{F}$ at the surface.

Note that for a large aperture S, Eq. (4) is transformed into a convolution-type integral and can approximately be written as

$$Q(\boldsymbol{\rho}_1, \boldsymbol{\rho}_\mathrm{F}, z_1, f) \approx Q(\boldsymbol{\rho}_\mathrm{F} - \boldsymbol{\rho}_1, z_1, f).$$

This allows us to approximately apply the instrument function found at one point for other points, as well. The most important parameter here is the quantity $\boldsymbol{\rho} \equiv \boldsymbol{\rho}_\mathrm{F} - \boldsymbol{\rho}_1$. The result of numerical calculation of the instrument function $Q(\boldsymbol{\rho}, z, f)$ in free space ($n = 1$) for the frequency $f = 10$ GHz, a synthetic aperture of 50 cm, and its height $h = 30$ cm is shown in Fig. 2*a*. Here, the darker parts of the plot correspond to higher amplitudes. Figure 2*b* shows the amplitude of the instrument function for a medium with the refractive index $n = 3$. It is seen that the region of the strongest system response to a point scatterer expands in the vertical direction with increasing refractive index n of the lower half-space. In other words, an increase

in the electrical phase increment of the wave relative to its geometrical-path length leads to a noticeable extension of the focus region in the lower medium.

It is important to emphasize that the performed focusing should ensure localization of inhomogeneities only in the horizontal direction, whereas the focusing in the vertical direction is not yet achieved in this stage. It is clear on general grounds that it would be more correct to choose the focus point directly in the bulk of the sounded medium. However, such focusing requires rather cumbersome calculations and consumes much longer time for the data processing, for example, up to 4 hours, as is mentioned in [1]. It is seen in Figs. 2*a* and 2*b* that the effect of refraction of waves extends the region of near-surface focusing into the depth of the medium. This effect is stronger for a larger refractive index n of the sounding medium.

3. THE STRONG-REFRACTION APPROXIMATION

Bearing in mind the large extension of the instrument function in the vertical direction, we assume that the refracted plane waves in the lower medium propagate perpendicular to the interface of the media. This approximation is better for a larger refractive index n of the sounded medium. Under this assumption, the expression for k_{1z} is simplified to $k_{1z} = \sqrt{k^2n^2 - k_\perp^2} \approx kn = k_1$, so that the factor $\exp(ik_1z)$ in Eq. (2) can be removed from the integral as follows:

$$G(\boldsymbol{\rho}, z) \approx \exp(ik_1z) \iint\limits_{-\infty}^{+\infty} \frac{iT(\mathbf{k}) \exp[i\,(\mathbf{k}_\perp\boldsymbol{\rho} + k_zh)]}{2\,(2\pi)^2\,k_z}\,\mathrm{d}^2\mathbf{k}_\perp \equiv \exp(ik_1z)G_\perp(\boldsymbol{\rho}). \tag{5}$$

Then one can write the instrument function

$$Q\,(\boldsymbol{\rho}_\mathrm{F} - \boldsymbol{\rho}_1, z_1, f) \approx k_1^2 \exp(2ik_1z_1) \iint\limits_S G_\perp^2(\boldsymbol{\rho}_1 - \boldsymbol{\rho}_0)M(\boldsymbol{\rho}_\mathrm{F} - \boldsymbol{\rho}_0, f)\,\mathrm{d}\boldsymbol{\rho}_0 \equiv \exp(2iknz_1)Q_\perp(\boldsymbol{\rho}_\mathrm{F} - \boldsymbol{\rho}_1, f).$$

Changing the order of integration in Eq. (3) and using Eqs. (1) and (5), we can write the focused field

$$F(\boldsymbol{\rho}_\mathrm{F}, f) = \int\limits_{-\infty}^{0} \exp(i\,2knz_1) \iint \Delta\varepsilon(\boldsymbol{\rho}_1, z_1)Q_\perp(\boldsymbol{\rho}_\mathrm{F} - \boldsymbol{\rho}_1, f)\,\mathrm{d}\boldsymbol{\rho}_1\,\mathrm{d}z_1, \tag{6}$$

where

$$Q_\perp(\boldsymbol{\rho}_\mathrm{F} - \boldsymbol{\rho}_1, f) = Q(\boldsymbol{\rho}_\mathrm{F} - \boldsymbol{\rho}_1, z_1 = 0, f) = \iint\limits_S M(\boldsymbol{\rho}_\mathrm{F} - \boldsymbol{\rho}_0, f)G_\perp^2(\boldsymbol{\rho}_1 - \boldsymbol{\rho}_0)\,\mathrm{d}\boldsymbol{\rho}_0$$

has the meaning of the transverse instrument function at frequency f. Figure 2*c* shows the calculated transverse instrument function $Q_\perp(\boldsymbol{\rho}, f)$ for the frequency $f = 10$ GHz. It is clear that this function coincides fairly well with the instrument function for the refractive index $n = 3$ up to a certain depth z_max beyond which the approximation becomes inapplicable. The extent of localization of the instrument function $Q_\perp(\boldsymbol{\rho}, f)$ over $\boldsymbol{\rho}$ determines the potential resolution of the system in the horizontal plane.

To estimate the applicability limits of the strong-refraction approximation, we turn to Fig. 3. First of all, we note that the formed focus region at the interface of the media has a finite width which is determined by the condition of deterioration of the phasing between the interfering waves in the direction towards the outer boundary of the focus region. It is known that for an aperture B, the transverse size of the focus region can be estimated approximately as

$$R \approx \lambda h/B,$$

where λ is the wavelength of the radiation. In our example, this quantity is about $R \approx 1.8$ cm, which agrees with Fig. 2. It is clear on physical grounds that the focus region in the lower half-space should extend in

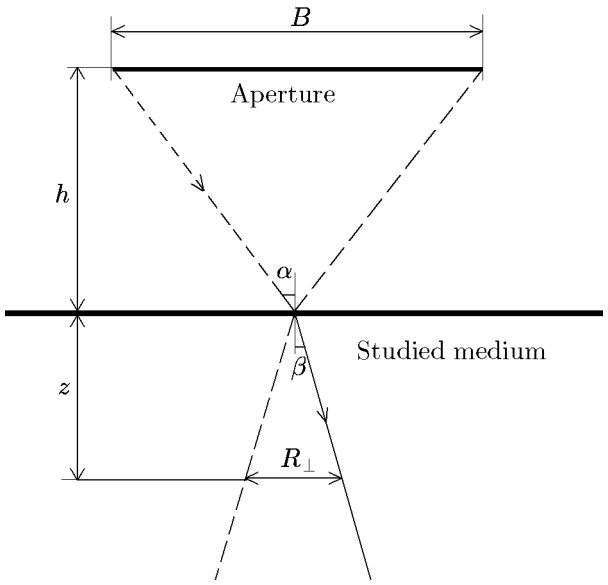

Fig. 3. Diagram for estimating the applicability limits for the strong-refraction approximation.

the transverse direction in such a way that the larger is the refractive index n, the smaller is the extension rate. We assume that the region of the wave-beam convergence to the focus point in the upper half-space is determined by the incidence angle α. Then it follows from the diagram shown in Fig. 3 that

$$\sin\alpha = 1/\sqrt{1+(2h/B)^2}.$$

The refraction angle β determines the divergence of the focus region in the lower half-space. The transverse divergence $R_\perp$ of the wave beam at a certain depth z is determined from the relationship

$$\sin\beta = 1/\sqrt{1+(2z/R_\perp)^2}.$$

One can consider this divergence insignificant if $R_\perp \le R$. Hence, taking into account that the incidence and refraction angles are related by the Snell's law $\sin\alpha = n\sin\beta$, we obtain the following expression for the depth $z_{\max}$ up to which the divergence can be neglected:

$$z_{\max} \equiv (\lambda h/(2B))\,\sqrt{n^2-1+(2nh/B)^2}. \tag{7}$$

For the case considered in Fig. 2*b*, Eq. (7) yields $z_{\max} \approx 4.1$ cm. This agrees with the results of the comparison between Figs. 2*b* and 2*c* which almost coincide up to a depth of 4.1 cm.

Let us make two notes. First, the above-adopted approximation is also valid for media with complex refractive indices, i.e., when the medium is absorbing. In such a case, based on the adopted simplifications, one can conclude that the absorption in the medium should not strongly affect the resolution of the method, but should decrease the limiting depth of detection of the inhomogeneities because of the attenuation of the waves in the medium. The limiting depth of the method workability is determined by the extinction depth $z_{\rm e} \approx (k\,\mathrm{Im}\,n)^{-1}$ at which the wave decays by a factor of e. This condition can be formulated as $z_{\max} \le z_{\rm e}$.

Second, the proposed strong-refraction approximation is not related to a particular polarization of the sounding wave, especially taking into account that below the interface, the wave propagates almost perpendicular to the boundary and the orthogonal polarizations are almost indistinguishable. In the general case, to take into account the polarization characteristics of the wave, it is sufficient to pass to the dyadic Green's function in Eqs. (1) and (2). In the considered case, the change in the polarization type affects only the amplitude characteristics via the Fresnel transmission coefficient.

4. THE INSTRUMENT FUNCTION IN THE STRONG-REFRACTION APPROXIMATION

Let us apply to Eq. (6) the Fourier transform over all frequencies for which the measurements are made. As a result, we obtain

$$\tilde F(\boldsymbol{\rho}_{\rm F},t) \equiv \int F(\boldsymbol{\rho}_{\rm F},f)\exp(-i\,2\pi f t)\,\mathrm{d}f = \iiint\limits_{V_1} \Delta\varepsilon(\boldsymbol{\rho}_1,z_1)\tilde Q_\perp\!\left(\boldsymbol{\rho}_{\rm F}-\boldsymbol{\rho}_1,\frac{ct}{2n}-z_1\right)\mathrm{d}\boldsymbol{\rho}_1\,\mathrm{d}z_1, \tag{8}$$

where

$$\tilde Q_\perp\!\left(\boldsymbol{\rho}_{\rm F}-\boldsymbol{\rho}_1,\frac{ct}{2n}-z_1\right) \equiv \int Q_\perp(\boldsymbol{\rho}_{\rm F}-\boldsymbol{\rho}_1,f)\exp[-i\,2\pi f\,(t-2nz_1/c)]\,\mathrm{d}f$$

is the instrument function of the system in the space-time domain. The numerical simulation for the frequency band from 0.5 to 17 GHz shows that the function $\tilde{Q}_\perp$ is localized in all three directions (Fig. 4). The calculation was made under the assumption that a point inhomogeneity is located at the depth $z_1 = 4$ cm.

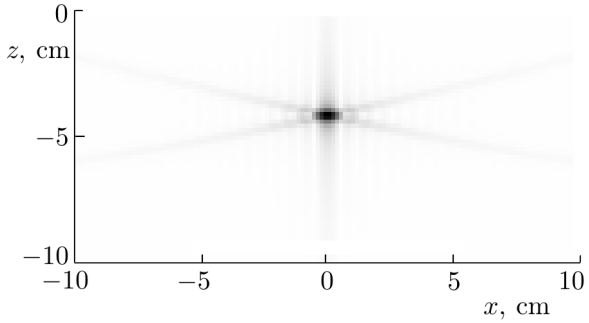

Fig. 4. Localization of the instrument function $\tilde{Q}_\perp(x, z)$ of the system.

Within the framework of the adopted approximations, for the spatial reconstruction of the inhomogeneities $\Delta\varepsilon(\boldsymbol{\rho}_1, z_1)$, it is sufficient to write the solution of the integral equation in convolution form (8). This is the well-known problem, which is usually solved using the Wiener filtering with regularization. However, the above-established fact of strong localization of the instrument function allows one to consider in a first approximation that

$$\Delta\varepsilon(\boldsymbol{\rho}_\mathrm{F}, z_\mathrm{F}) \propto \tilde{\mathrm{F}}(\boldsymbol{\rho}_\mathrm{F}, 2nz_\mathrm{F}/c) = \int\limits_{-\infty}^{+\infty} \exp(-i\,2knz_\mathrm{F}) \iint\limits_S E(\boldsymbol{\rho}_0, f) M(\boldsymbol{\rho}_\mathrm{F} - \boldsymbol{\rho}_0, f)\,\mathrm{d}^2\boldsymbol{\rho}_0\,\mathrm{d}f. \tag{9}$$

The accuracy of resolution in this case is determined by the localization scale of the instrument function.

In view of the adopted approximations, the solution of the inverse problem of subsurface tomography is reduced to focusing of the radiation to a near-surface point of the medium and application of the inverse Fourier transform in the frequency domain. Note that the focusing does not require *a priori* information on the refractive index of the medium. Application of the FFT algorithm makes it possible to significantly fasten the measurement-data processing.

5. EXPERIMENTAL STUDIES

To test the workability of the proposed method for reconstruction of the distribution of inhomogeneities, we carried out two experiments. In the tests, we used sand as the medium. In the first experiment, two metal corner reflectors with a facet size of 5 cm were placed at depths of 9 and 10 cm. We used frequency range 0.5–17 GHz. After processing of the measurement data using Eq. (9), we obtained the image presented in Fig. 5. The reconstructed image shows that the scattering objects can unambiguously be distinguished both in the vertical and horizontal directions. Comparison between the measured time delay of the signals and the actual depths of the scatterers made it possible to more precisely evaluate the sand refractive index, $n = 1.5$.

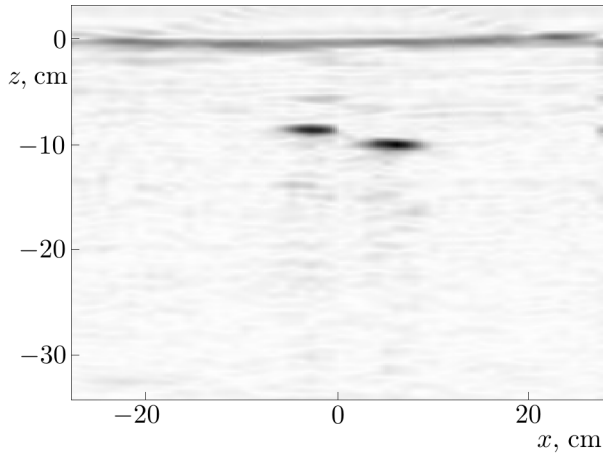

Fig. 5. Radio-tomographic image of corner reflectors. The darker regions correspond to greater values of $\tilde{F}$.

The second experiment was carried out with four test dielectric objects placed at different depths. At the depths between 1 and 25 cm, we placed three plastic cases of antipersonnel mines and a test object prepared from foamed polystyrene and having a stepwise shape with a step dimension of 5 cm. The picture of these objects is shown in Fig. 6. In the measurements, we used the frequency range 0.5–17 GHz. A system of the receiving and transmitting antennas with a 14 cm fixed separation was moved in 1-cm steps in the horizontal plane within a square region of 50×50 cm at a height of 30 cm over the sand surface.

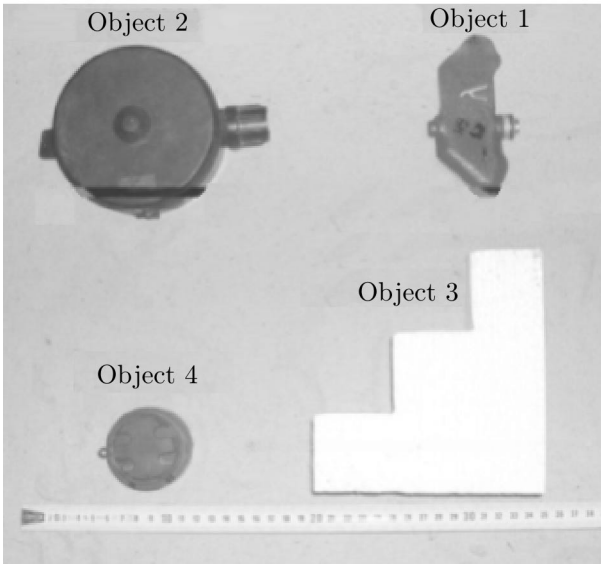

Fig. 6. Test objects.

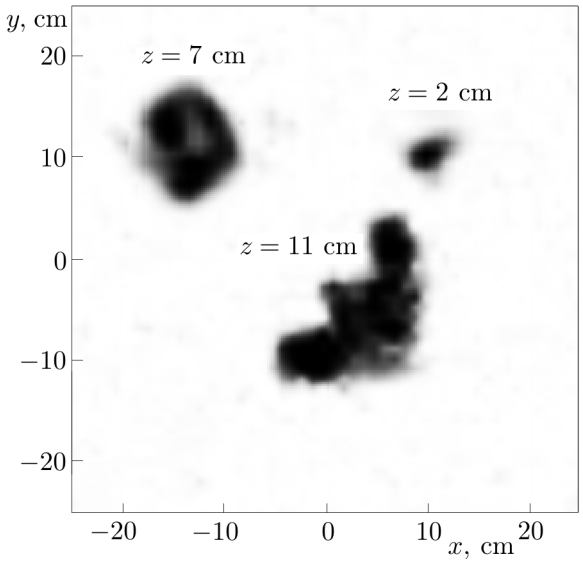

Fig. 7. The reconstructed image of the spatial distribution of the inhomogeneities.

The result of reconstructing the shapes and location of the test objects is shown in Fig. 7. To improve the visual quality of the image, linear filtering of the signal was used with increasing amplitude at higher spatial frequencies.

The presented images show that the proposed method and the described setup ensure the resolution about 1 cm up to a depth of 11 cm. Object *4* buried at a depth of 25 cm was not detected, which was related to the attenuation of the signal in the medium and the divergence of the instrument function at the larger depths.

6. CONCLUSIONS

In this work, we proposed a method for reconstruction of buried heterogeneities on the basis of the synthetic-aperture radar technique. The method uses data of ultra-wideband radio-wave sounding and ensures the real-time processing of these data. Results of numerical calculation of the instrument function and the resolution estimates for the proposed system are presented. It is shown that in the approximation of a strongly refractive medium, the use the ultra-wideband radiation ensures a reasonable resolution in the medium bulk by focusing of the scattered field only to the near-surface points of the medium. An estimate is presented for the maximum depth of the method applicability in the case of finite values of the refractive index.

The proposed method for imaging the inhomogeneities has a high processing speed due to the possibility of using the FFT. The theoretical results are corroborated by the data of model experiments on the tomographic reconstruction of dielectric inhomogeneities buried in the sand. It is shown that the use of sounding frequencies in the range 0.5 – 17 GHz ensures the reconstruction of the object shapes with a resolution of about 1 cm for depths of up to 11 cm.

Experimental studies were carried out in the laboratory of the Department of Microwave and Communication Engineering in the Institute for Electronics, Signal Processing, and Communications at the Faculty of Electrical Engineering and Information Technology of the Otto-von-Guericke University of Magdeburg, Magdeburg, Germany. The authors are grateful to Prof. A. S. Omar and the authorities of the University of Magdeburg for the provided possibility of the experimental studies.

This work was supported by the program "Universities of Russia" (project No. UR.01.01.395, 2005) and the program of the Russian Federal Agency of Science and Innovations (project No. 2005-RI-16.0/013).

REFERENCES

1. J. Fortuny-Guasch, *IEEE Trans. Geosci. Remote Sensing*, **40**, No. 2, 443 (2002).
2. S. Valle, L. Zanzi, H. Lentz, and H. M. Braun, in: *8th Int. Conf. Ground Penetrating Radar*, 2000, p. 464.
3. I. L. Morrow and P. van Genderen, *IEEE Trans. Geosci. Remote Sensing*, **40**, No. 4, 943 (2002).
4. J. Groenenboom and A. G. Yarovoy, in: *8th Int. Conf. Ground Penetrating Radar*, 2000, p. 367.
5. A. H. Gunatllaka and B. A. Baertlein, *Detection and Remediation Technologies for Mines and Minelike Targets V*, 1008 (2000).
6. P. Meincke, in: *Proc. 10th Int. Conf. on Ground Penetrating Radar*, 2004, p. 55.
7. V. P. Yakubov, A. S. Omar, V. P. Kutov, et al., in: *10th Int. Conf. on Ground Penetrating Radar*, 2004, p. 103.
8. M. M. Golovko and G. P. Pochanin, *Electromagn. Wolny Electron. Syst.* **9**, Nos. 9–10, 22 (2004).
9. L. M. Brekhovskikh, *Waves in Layered Media*, Academic Press, New York (1960).